Flexural Behavior of One-Way Slabs Reinforced with Welded Wire Mesh under Vertical Loads

El-Sayed S. Ewida [1], Rasha T. S. Mabrouk [1*] , Nasser El-Shafey [1], Akram M. Torkey [2]

[1] *Structural Engineering Department, Cairo University, Cairo, Egypt.*

Abstract

This paper aims to study the behavior of one-way concrete solid slabs reinforced with welded wire mesh to investigate the efficiency of using welded wire mesh in the construction of structural slabs as a replacement for ordinary steel bars. This research included experimental and analytical programs. Nine 700×1050 mm one-way simple specimens and six 525×1050 mm continuous one-way slabs with two equal spans were tested under point, line, and uniform static loads. The experimental program studied the use of welded mesh and the number of layers utilized. Numerical analysis was conducted using finite element modeling developed using the ABAQUS 6.13 software package. Experimental and analytical results showed good correlation: the number of layers of welded metal mesh and load type significantly affected the peak vertical load capacity of simple and continuous slabs, with slabs showing higher values with welded mesh than those of ordinary reinforcing bars. In addition, using welded metal mesh to reinforce solid slabs enhanced their cracking behavior as well as their ductility.

Keywords: Welded Metal Mesh; One-Way Slabs; Crack; Deflection; Ductility; Abaqus.

1. Introduction

Welded wire steel mesh provides a convenient and economical alternative to ordinary reinforced steel bars in concrete structures. More speed and better quality, together with cost reduction, are essential elements in construction development. Using welded wire mesh can satisfy these requirements. According to the ACI PRC-439.5-18 [1], "Welded Wire Reinforcement (*WWR*) is prefabricated reinforcement consisting of high-strength cold-worked steel wires that are resistance-welded together in square or rectangular grids by continuous automatic welders." Welded meshes are available in various sizes and shapes, and the mesh bars can be specially coated to improve their surface resistance to chemicals and other corrosive substances.

Naser et al. (2021) [2] experimentally studied the effect of using different types of reinforcement on the flexural behavior of ferrocement thin hollow core slabs with embedded PVC pipes. Twelve 1100×400×55 mm specimens were cast and tested to failure. The study included steel wire mesh, macro and micro steel fibers, or a combination of both, steel bars, and CFRP bars. Results showed that using wire mesh layers at the compression zone of a thin hollow core slab considerably increases the ultimate flexural strength and stiffness of the slab when compared with that reinforced with wire mesh at the tension zone only. However, and in general, slabs reinforced with wire mesh exhibit lower flexural strength and stiffness when compared with the other types of reinforcement. The slab reinforced with only macro steel

fibers provided the highest flexural strength, while the slab reinforced with steel bars showed the highest stiffness and lowest deflection among all tested slabs.

In another work, Ali et al. (2020) [3] investigated the use of thin mortar matrix for the impact of a combination of reinforcing steel meshes with discontinuous fibers. To do this, one-way ferrocement slabs were tested under bending with steel fibers and meshes, focusing more on the number of mesh layers (1, 2, & 3) as the studied parameter. Results showed that adding fibers, regardless of their type, increased the ductility of tested slabs. In addition, it was shown that the increment of wire number of mesh layers and distribution along the thickness of the slab results in a higher strength capacity and more ductile behavior. Also, steel fibers are more effective than aluminum fibers.

Allawi & Ali (2020) [4] performed a behavioral study on ferrocement slabs under flexural loading and punching shear strength between chicken and square welded mesh. They assessed parameters in their study, including effects of volume fraction, panel thickness, and load-deflection relationship. Results showed that the failure pattern and cracking behavior of the ferrocement slab were related to volume fraction and type of reinforcement. Load carrying capacity and flexural load increased with an increase in mesh diameter and maintaining the proper space between two mesh layers. Leeanansaksiri et al. (2018) [5] noted that ferrocement can be used in different applications due to its properties, such as precast units. Additionally, ferrocement is lighter than traditional concrete by up to 70%, which can be suitable for low-cost housing. Unfortunately, a scarcity of research can be found on the use of welded mesh with ordinary concrete. In one study, Li et al. (2018) [6] compared conventional RC slabs with the replaced welded mesh slabs to develop a high strength concrete by testing the mechanical properties and strength variations between them. Experimental results showed that the difference between the flexural behavior of both conventional and welded mesh slabs is that they have two continuous cracks with a 0.5 mm width traveling up to the top of the slab.

In another study, Shaheen et al. (2018) [7] examined the effect of reinforcing ordinary concrete with welded metal mesh on the behavior of slabs with openings under impact loadings. They found that adding expanded mesh resulted in fewer displacement values than employing welded mesh. The difference, in some cases, reached 24.3%. Specimens reinforced with metal mesh had smaller cracked zones compared to their counterparts without metal mesh. Cracking spread decreased significantly in specimens reinforced by expanded metal mesh.

Moreover, Yousry & Eltehawy (2017) [8] present a new pre cast U-shape ferrocement form reinforced with various types of metallic and non-metallic mesh reinforcement. This research was designed to investigate the feasibility and effectiveness of employing various types of reinforcing meshes in the construction of structural slabs incorporating permanent U-shape ferrocement forms as a viable alternative to conventional reinforced concrete slabs. Fiber glass mesh reinforcement was used for durability and protection against corrosion of the reinforcing steel. An experimental program was conducted to accomplish this objective. The experimental program comprised casting and testing ten slabs having a total dimension of 500x100x2500 mm, incorporating 40 mm thick U-shape permanent ferrocement forms. The results show that employing welded galvanized steel mesh gave the highest results compared to all tested U-shaped slabs. Using two to four layers of welded galvanized steel mesh in reinforcing ferrocement U-shaped slabs improves the energy absorption compared to that obtained when using skeletal steel bars.

However, little research can be found on the use of welded mesh with ordinary concrete. This research aims to study the behavior of solid slabs reinforced using welded wire mesh. Generally, the use of welded wire mesh improves concrete behavior. It provides a good distribution of steel reinforcement throughout the concrete slab, due to the larger number of small diameter wires, which are closely and more uniformly distributed. In addition, welded wire mesh shows smaller crack spacing and crack width compared to conventional reinforcing bars. The welded mesh enables the use of smaller cross sections for the concrete elements. Furthermore, steel bars rely entirely on the adhesion of the concrete to the bar surface to provide bond for anchorage. For the welded wire mesh, mechanical anchorage is utilized through the rigidly connected wires welded at their intersection. There are many other advantages to using welded wire mesh, such as improving the construction site efficiency and productivity as there is a reduced reliance on manpower on-site, as well as providing speedy construction where the welded mesh can be placed in a position relatively faster compared to placing individual bars and tying them in place. At the same time, less storage space is needed.

1.1. Research Significance

This research studies the structural behavior of one-way solid slabs reinforced with welded wire metal mesh under point, line, and uniform loads to investigate the effect of using this type of reinforcement compared to using ordinary steel bars. The slabs were chosen with small spans, which are relevant to the low-cost housing currently used in the rapid construction in Egypt. An experimental program was carried out on simple and continuous one-way reinforced slabs using one and two layers of welded mesh in addition to ordinary steel bars. Following that, a finite element model, using the software package ABAQUS, was conducted to investigate the tested specimens, and a comparison was made with the experimental data obtained. Figure 1 shows the flowchart of the research methodology.
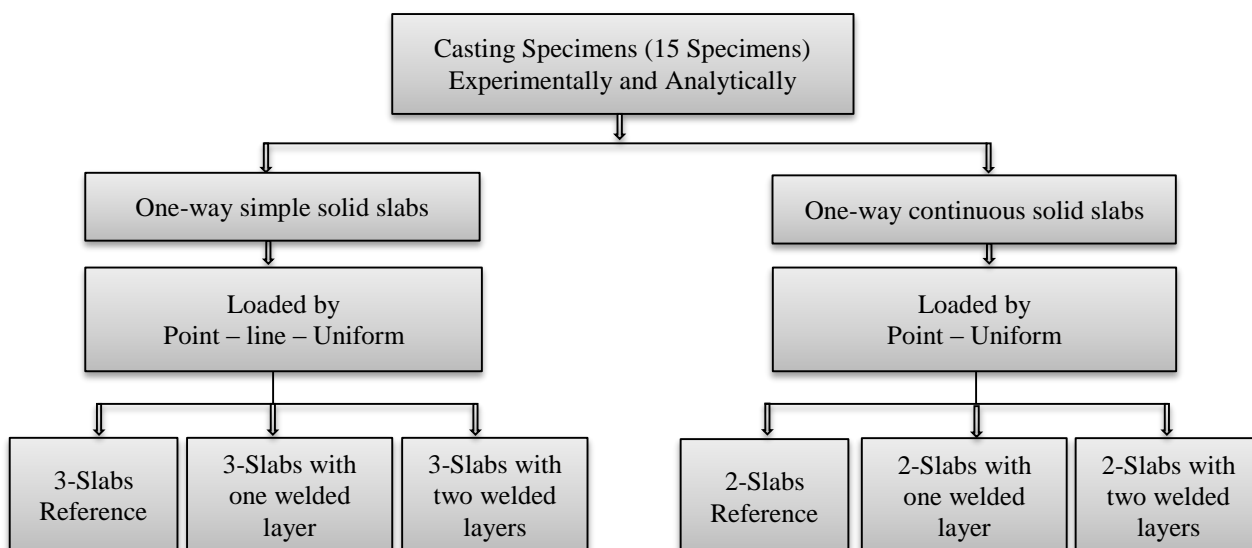
Figure 1. Flowchart for research methodology

2. Experimental Program

The experimental program comprised casting and testing fifteen slabs divided into five groups at the Concrete Research Laboratory, Faculty of Engineering, Cairo University. All the tested one-way specimens had the same dimensions of 700×1050 mm and 50 mm thickness, while the continuous specimens had the same thickness with two equal spans of dimensions 525×1050 mm. Thickness of 50 mm is the minimum thickness that can be taken on the experimented slabs casted by ordinary concrete with concrete cover equal to 15 mm. One conventionally reinforced concrete slab in every group was cast and tested as a control specimen. The test parameters were the number of welded metal mesh and load type, in addition to the continuity of slabs. Tables 1 and 2 show the notation used to refer to each specimen. The letter R refers to the control specimen reinforced with ordinary bars; the letter F refers to the specimen having welded-mesh; the letter S or C defines the solid slab type where S is for simple and C is for continuous, and the number following the letter S or C refers to the number of metal-mesh in each direction. CL refers to concentrated load, LL refers to line load, and UL refers to uniform load.

Table 1. Simple one way slab identification notation and details

Group No.	Specimens	Group No	Specimens	Group No	Specimens	Type of RFT Mesh	RFT (Φ mm)	F_y (MPa)
Group 1 Point Load	RO-S0-CL	**Group 2 Line Load**	RO-S0-LL	**Group 3 Uniform Load**	RO-S0-UL	Steel bar mesh	Φ8@142	368
	FO-S1-CL		FO-S1-LL		FO-S1-UL	One welded mesh layer	FΦ5@50	418
	FO-S2-CL		FO-S2-LL		FO-S2-UL	Two welded mesh layers	FΦ5@50+Add Φ5@50	418

Table 2. Continuous one-way slab identification notation and details

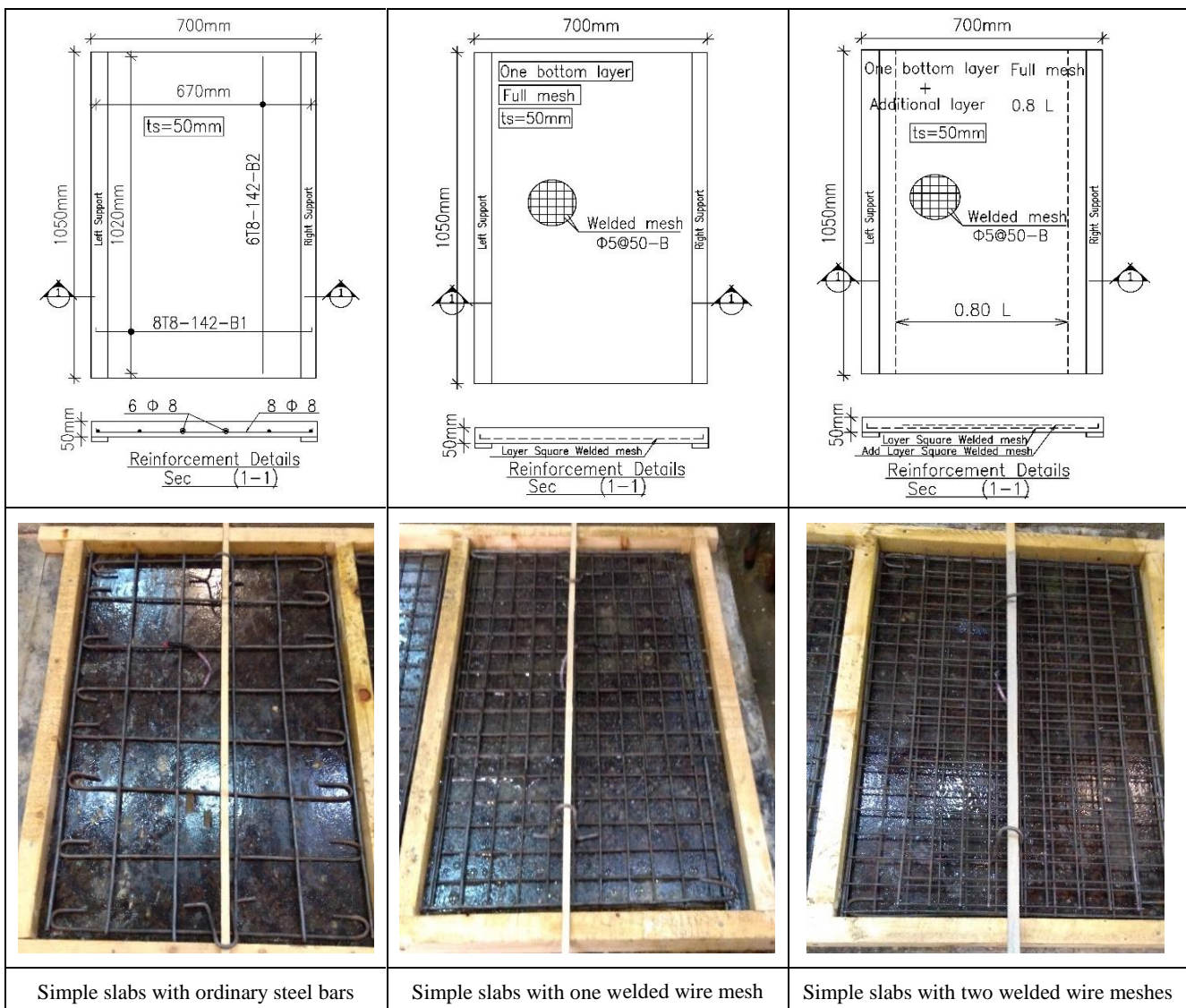| Group No.	Specimens	Group No.	Specimens	Type of RFT Mesh	RFT Φ mm	Fy MPa
Group 4 Point Load	RO-C0-CL	**Group 5 Uniform Load**	RO-C0-UL	Steel bar	Φ8@142	368
	FO-C1-CL		FO-C1-UL	One welded mesh layer	FΦ5@50	418
	FO-C2-CL		FO-C2-UL	Two welded mesh layers	FΦ5@50+Add Φ5@50	418

2.1. Material Properties

Ordinary Portland cement type CEM I 42.5N according to the requirements of E.S.S.4756-11 (2012) [10] with a specific gravity of 3.15 and a specific surface area (Blaine fineness) 3700 cm^2/g and 400 kg/m^3 content was used. Mild steel Φ 8 with yielding stress from laboratory testing equal to 368 MPa was provided by the national companies. The data sheet for welded mesh bars is listed in Table 3. The concrete mix was designed to give a compressive strength of 35.0 N/mm^2 after 28 days. A normal weight dolomite with a maximum size of 10 mm and a bulk density of 1680 Kg/m^3 was used as a coarse aggregate. The fine aggregate was normal sand. The mix proportion was 1:1.8:3.6 (cement to sand to dolomite) with a free water cement ratio of 0.50 and super plasticizer addicrete BVD777 was added. Two batches of concrete were used. One of them was used in groups 1 and 2, and the other was used in group 3. Results for the compressive strength of the concrete cubes for batch 1 is 36.3 N/mm^2 after 7 days and 42.06 N/mm^2 after 28 days, while batch 2 gives 39.18 N/mm^2 after 7 days and 44.26 N/mm^2 after 28 days.

Table 3. Manufacturer Data Sheet for Welded Metal Mesh

Property	Manufacture Data Sheet	(E.S.S, 1109,1971) limits	
Actual diameter	5.00	-------------	
Yield stress	418 kN/mm^2	Not less than 240 kN/m^2	
Ultimate stress	613 kN/mm^2	Not less than 480 kN/m^2	
Elongation	20.0 %	Not less than 20%	

2.2. Details of Specimens

The specimens were divided into five groups with a total of 15 slabs tested. Three groups were used for simple supported slabs and two groups for the continuously supported slabs. The first three groups had dimensions of 700×1050 mm and 50 mm in thickness, and the other two groups had two equal spans each of 525×1050 mm and 50 mm in thickness. Each group contained three slabs with one control specimen reinforced with ordinary steel bars, with the total number of bars equalling 8 as shown in Figure 2. The second specimen was reinforced with one layer of welded metal mesh with dimensions 50×50 mm and 5 mm bar diameter welded in both directions, with the total number of bars within the mesh = 18 as shown in Figure 2. The third specimen had two layers of welded mesh. The same reinforcement ratio was chosen for ordinary bars and for specimens with one layer of the welded mesh, with a reinforcement ratio of about 0.80% for slabs with ordinary steel bars, about 0.70% for slabs with one welded metal mesh, and 1.41% for the specimens with a double mesh layer. Figure 2 shows the concrete dimensions and reinforcement of the different specimens.
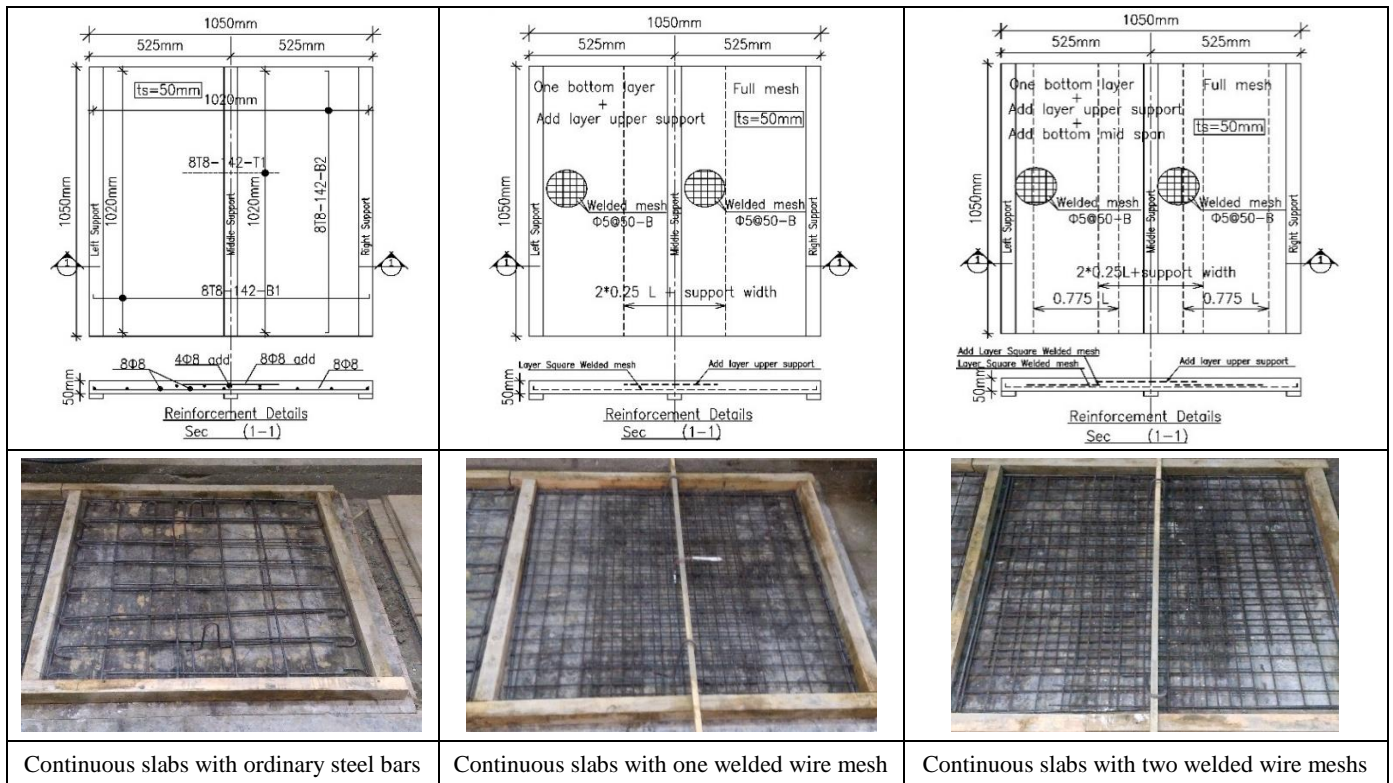
Simple slabs with ordinary steel bars	Simple slabs with one welded wire mesh	Simple slabs with two welded wire meshes

| Continuous slabs with ordinary steel bars | Continuous slabs with one welded wire mesh | Continuous slabs with two welded wire meshs |

Figure 2. Reinforcement details for different specimens

2.3. Test Setup

The test was conducted under different vertical loads as shown in Tables 1 and 2. Loading distribution for different types of loading was applied using wooden cubes (100×100×50 mm) in a laboratory. For line load, wooden cubes spaced every 100 mm along the loading line were used, while for uniform load, wooden cubic placed in both directions and spaced every 100 mm were arranged in a pyramid shape using steel channel beams to distribute the jack load uniformly to the top slab surface. Figures 3 and 4 show the test setup for the different specimens.
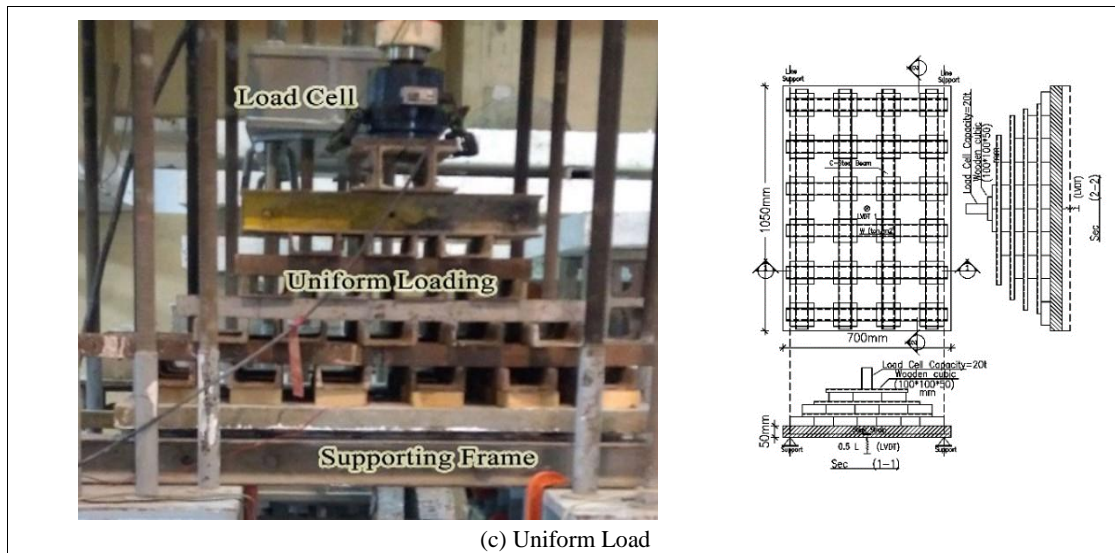

(a) Concentrated Load

(b) Line Load

(c) Uniform Load
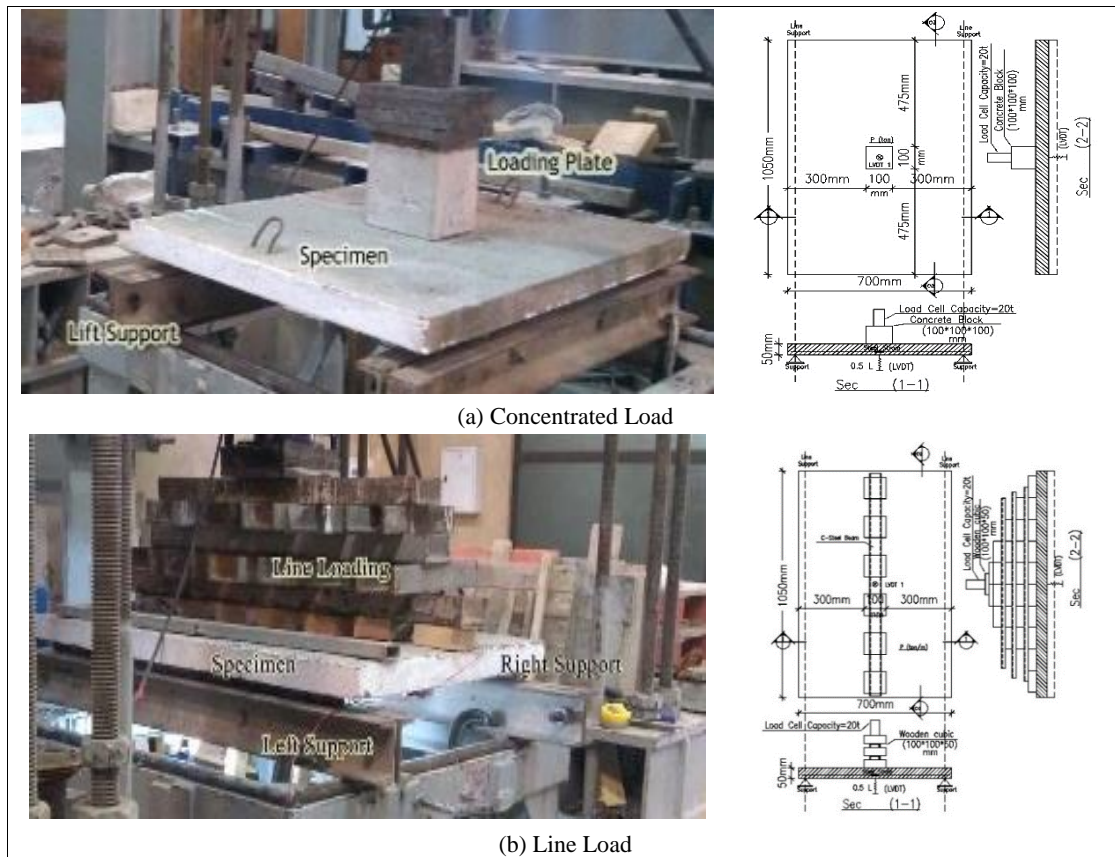
Figure 3. Test setup for simple supported slabs under different loads

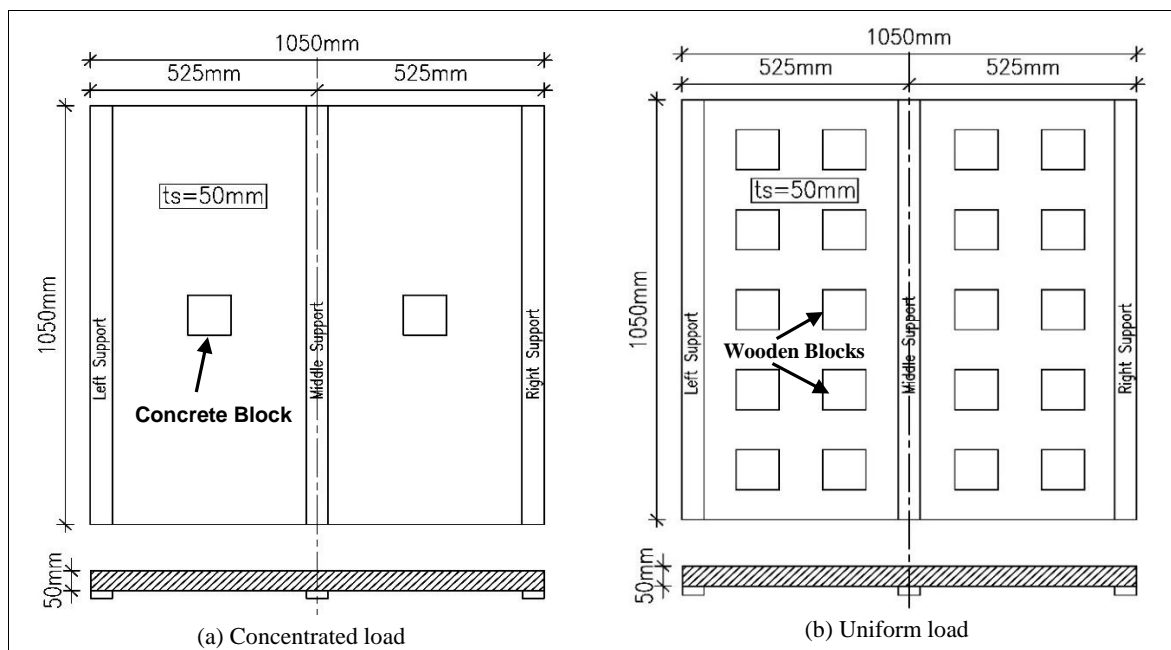(a) Concentrated load   (b) Uniform load

Figure 4. Test setup for continuous supported slabs under different loads

2.4. Modes of Failure and Cracks Pattern

The flexural failure is characterized by a smooth decrease of the carrying load with increasing displacement. Flexural failure is considered to take place in slabs in which most of the reinforcement yields; consequently, the slabs exhibit large deflection prior to failure. Flexural failure was observed in most of the specimens. However, there were two specimens where punching failure was observed. As shown in Figures 6 and 7, the cracking patterns for the slabs reinforced with welded mesh showed a larger number of cracks distributed along the bottom surface of the specimens, with smaller crack widths than the case of ordinary reinforcing bars. This shows a significant improvement in the cracking behavior when using welded mesh.

Group 1 comprised of simple specimens subjected to concentrated load. The cracks began under load and grew towards the slab parameter in a radial pattern as shown in Figure 6. For the specimen reinforced with ordinary bars, RO-S0-CL, one major crack appeared in the middle slab span, and by increasing the load, the crack width increased till the slab failed by flexural. Large spacing was observed between cracks due to the large spacing between bars, which was 142 mm. For the second specimen, FO-S1-CL, the spacing between cracks decreased with better distribution than RO-S0-CL due to the low spacing between welded mesh, which was 50 mm in both directions. This specimen also failed in flexural behavior. By adding an additional welded metal mesh layer in specimen FO-S2-CL, tensile strength was improved for concrete, and crack width was noticeably decreased with a larger number of cracks observed.

Group 2 comprised of simple specimens subjected to line load. The crack distribution in different specimens followed a rather linear pattern parallel to the line load applied. For specimen RO-S0-LL, two district parallel cracks were observed, while for specimen FO-S1-LL, one crack parallel to the line load was observed. The number of cracks increased, covering the whole surface of the specimen in the case of the specimen with a double mesh, FO-S2-LL. All specimens in this group failed in flexural.

Group 3 comprised of simple specimens subjected to uniform load. The cracks distribution on the bottom surface of the slab showed cracks parallel to the longitudinal side of the slab. Specimens RO-S0-UL showed a small number of cracks and failed due to flexure. Specimens FO-S1-UL and FO-S2-UL showed a more uniformly distributed crack pattern with FO-S2-UL showing more cracks with a smaller width than FO-S1-UL. Both specimens failed due to the crushing of concrete at the supports as shown in Figure 6. The two specimens exhibited extensive deformation after the peak load. This can be due to the formation of an arch action that transferred loads directly to the supports under the uniform loading conditions adapted. Loading was transferred from the loading jack to the top surface of the slab through wooden blocks. Steel channels were placed between the layers of wooden blocks which were a rigid structure and the increased deflection of the slabs caused the load to transfer directly from the loading point to the support.

Group 4 comprised of continuous specimens subjected to concentrated load as shown in Figure 7, the cracks distribution in specimen RO-C0-CL was in the form of distinct cracks starting under the point load and extending in two perpendicular directions. Specimens FO-C1-CL and FO-C2-CL failed due to punching failure. Due to the decrease in the slab span as well as the continuity, the slab carrying load capacity increased significantly and the failure changed from flexural to punching failure.

Group 5 comprised of continuous specimens subjected to uniform load. Uniform load distributed on the top slab surface was formed of two rows of wooden blocks thus the slabs acted similar to slabs loaded by two rows of line loads with small span width. The cracks distribution in different specimens followed the same pattern as the third group loaded under uniform load. Short span length and slab continuity increased the carrying load capacity of the slabs.

2.5. Load Deflection Behavior

Analysis and comparison were conducted between the results of the different test specimens to examine the effect of the test parameters under investigation. Figure 5 shows the load-deflection curves for all specimens and Table 4 shows the test results of the different groups.
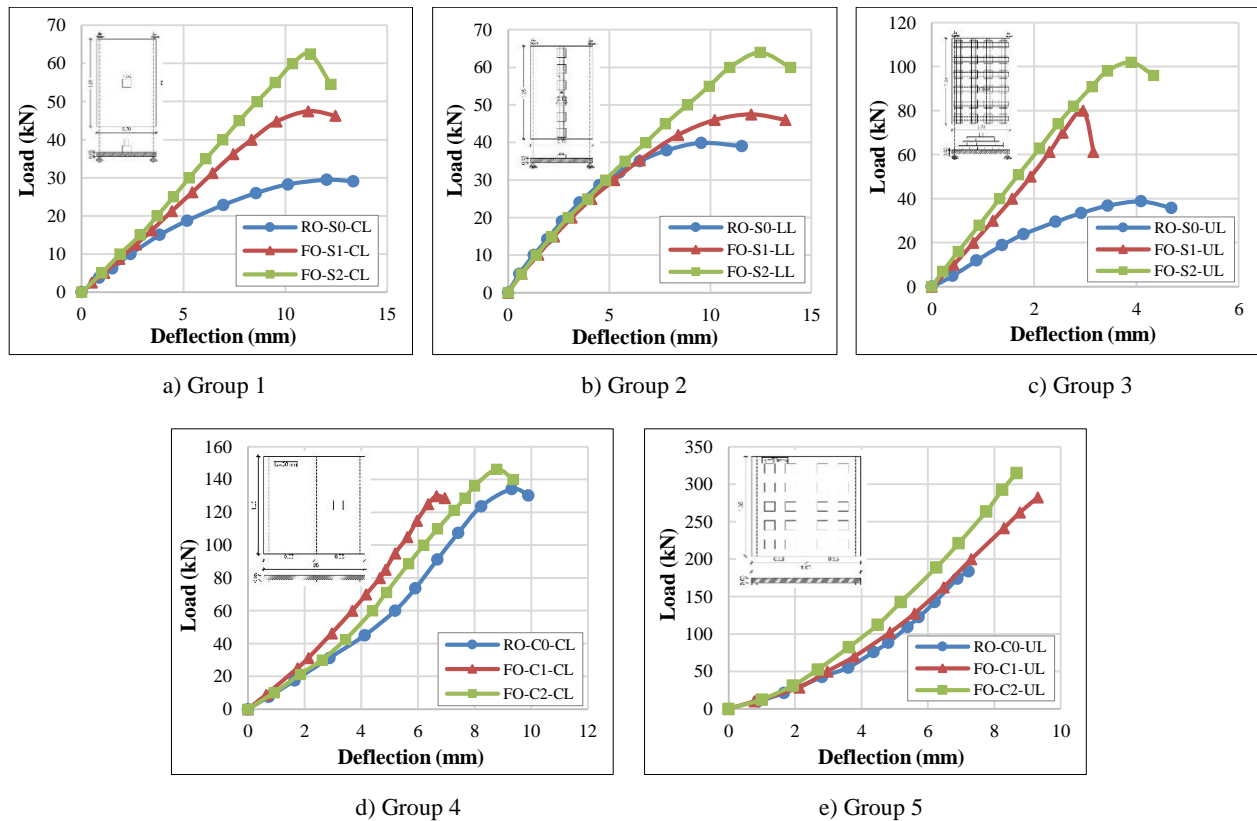

| a) Group 1 | b) Group 2 | c) Group 3 |

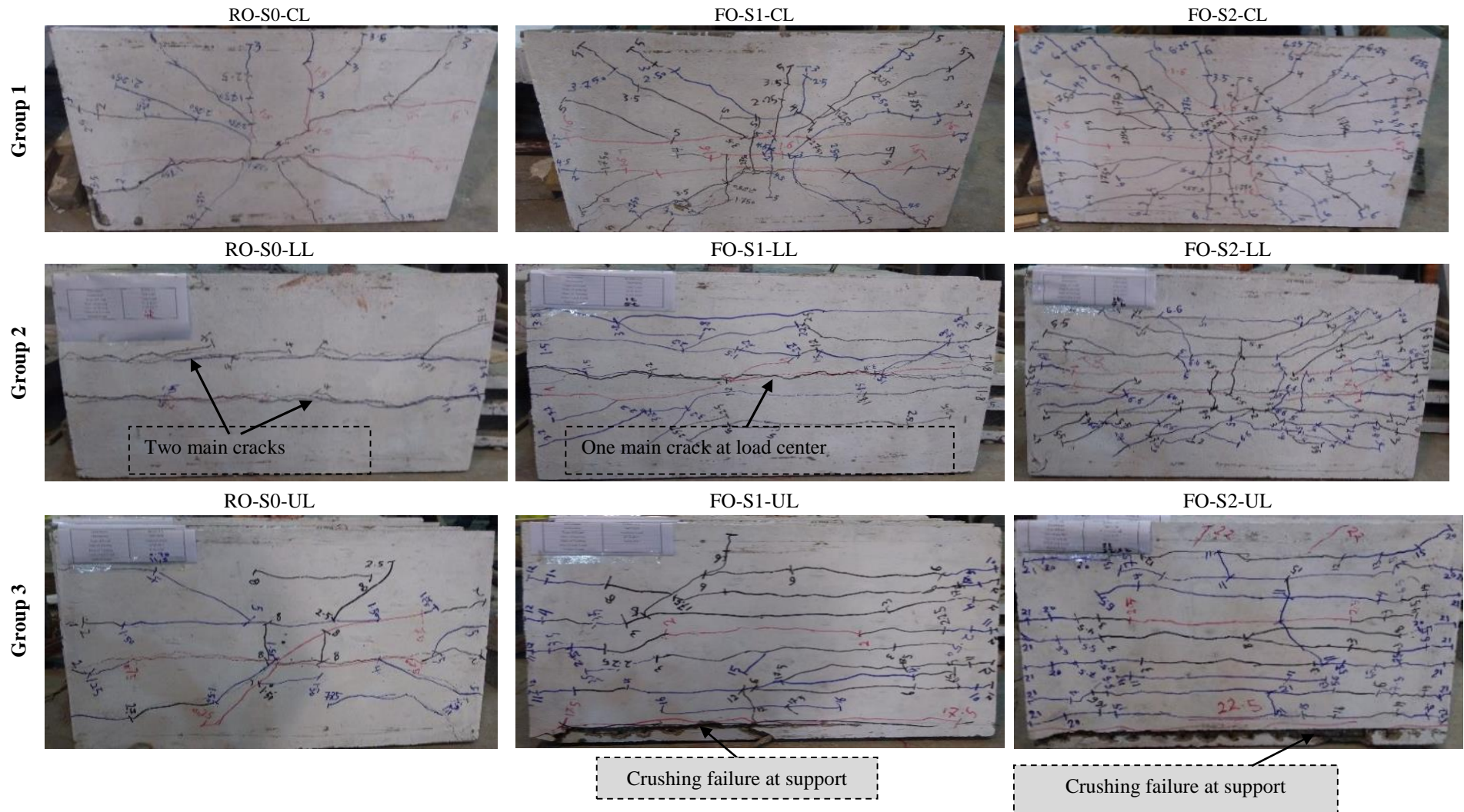
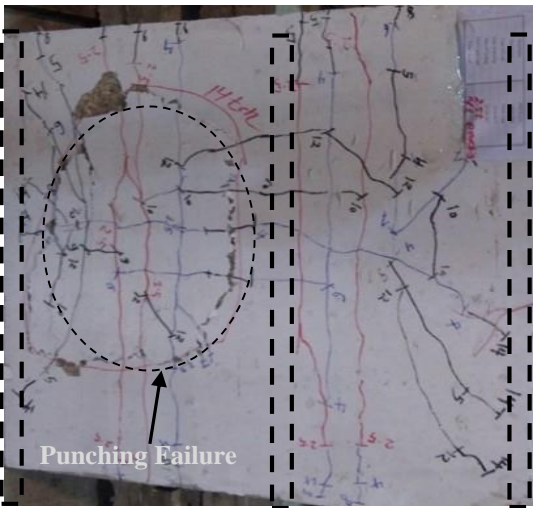| d) Group 4 | e) Group 5 |

Figure 5. Load–deflection curves for all specimens

Figure 6. Crack patterns for simple slabs specimens
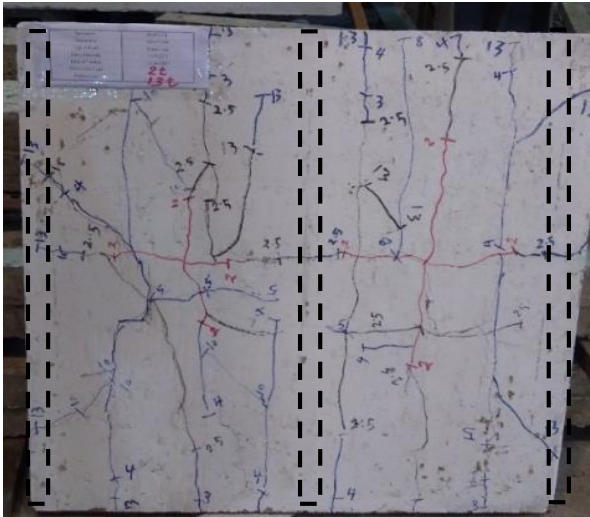
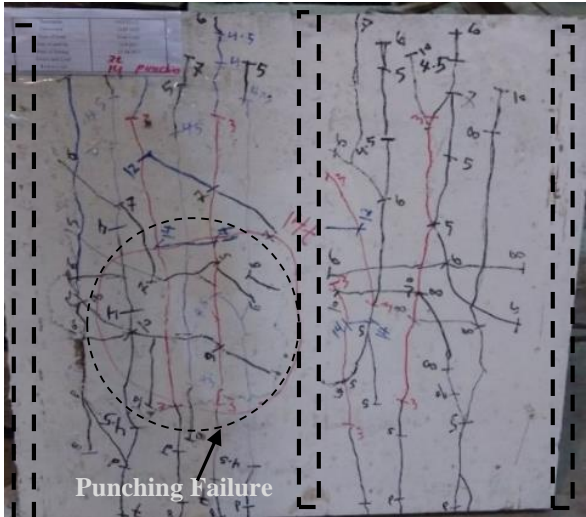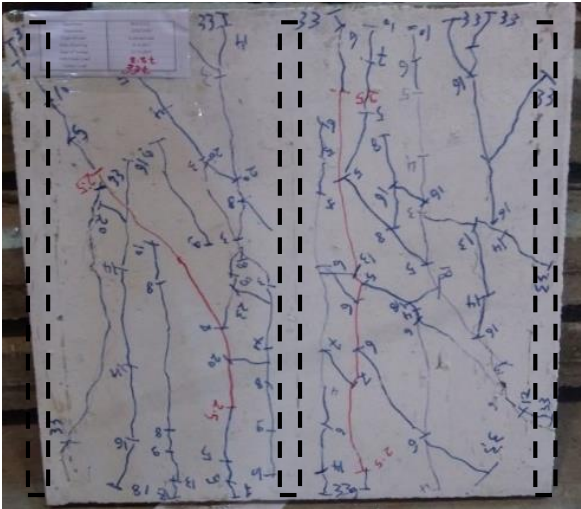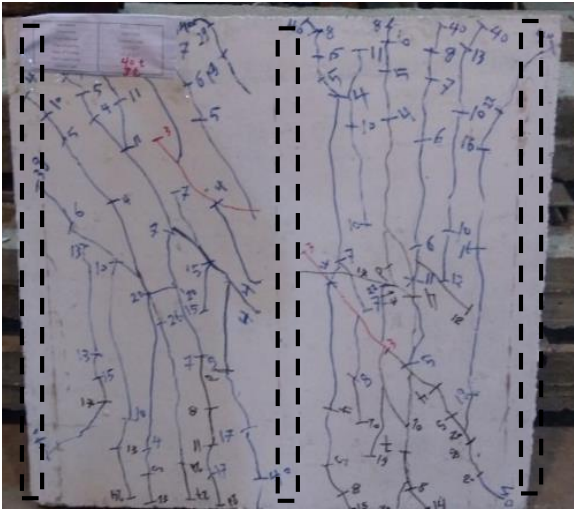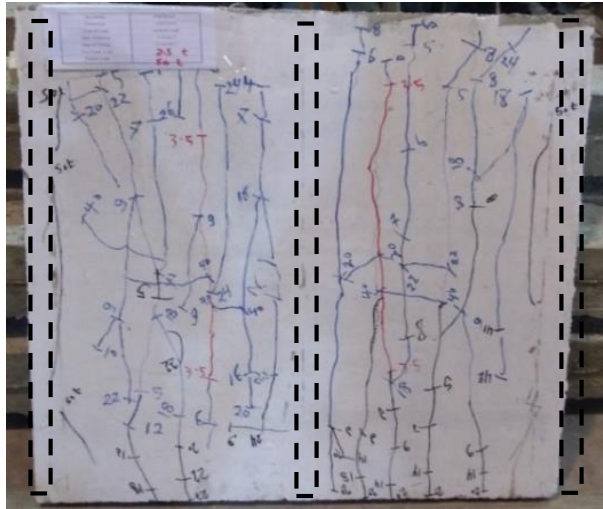**Figure 7. Crack patterns for continuous slabs specimens**

Table 4. Test results of different groups

Group No	Test Slab Designation	P_cr (kN)	Δ_cr(mm)	P_Ultimate (kN)	Δ_Ultimate (mm)	Ultimate Steel Strain /10⁶
Group 1	RO-S0-CL	15	3.83	29.42	12.02	1500
	FO-S1-CL	16	3.39	47.46	11.12	4500
	FO-S2-CL	16	3.06	62.45	11.22	3800
Group 2	RO-S0-LL	9.99	1.26	39.86	9.55	2500
	FO-S1-LL	10	1.47	47.46	12.02	2800
	FO-S2-LL	10	1.36	64.94	12.45	3300
Group 3	RO-S0-UL	7.50	0.54	38.76	4.08	2200
	FO-S1-UL	20	0.81	79.93	2.95	1900
	FO-S2-UL	20	0.64	101.91	3.89	2100
Group 4	RO-C0-CL	20	1.89	134.18	9.31	2200
	FO-C1-CL	25	1.75	129.93	6.65	1600
	FO-C2-CL	30	2.61	146.17	9.35	1000
Group 5	RO-C0-UL	25	1.96	183.65	7.23	2600
	FO-C1-UL	30	2.22	282.35	9.31	2300
	FO-C2-UL	35	2.18	314.84	8.67	1700

P_{cr} = First crack load, $P_{ultimate}$ = Ultimate load. Δ_{cr} = Deflection at first crack load, $\Delta_{ultimate}$ = Ultimate deflection.

For simply supported specimens (Groups 1 to 3), the load deflection curves were found to be linear up to the first crack load and then non-linearity was observed until failure. The first crack load had almost the same value for all the specimens under concentrated and line loads. However, for the ultimate load, specimens FO-S1-CL and FO-S2-CL showed an increase of 61% and 112% for one layer and two layers of mesh compared to the control specimen RO-S0-CL, while an increase of 19% and 63% was seen for specimens FO-S1-LL and FO-S2-LL. Figures 8 and 9 show the relative increase in the values of loads and deflections compared to control specimens in each group. For specimens subjected to uniform loads (Group 3), specimens reinforced with welded wire mesh showed a significant improvement in the values of both the first crack load and the ultimate load. Under uniform load, the grid action introduced through the presence of the welded wire mesh in both directions effectively enhanced the slab capacity. In addition, the arch action, explained earlier, can also add to the increase observed in the first crack and ultimate load values. It should be noted that excessive data recorded after the peak load was excluded from the figures and tables for specimens FO-S1-UL and FO-S2-UL.
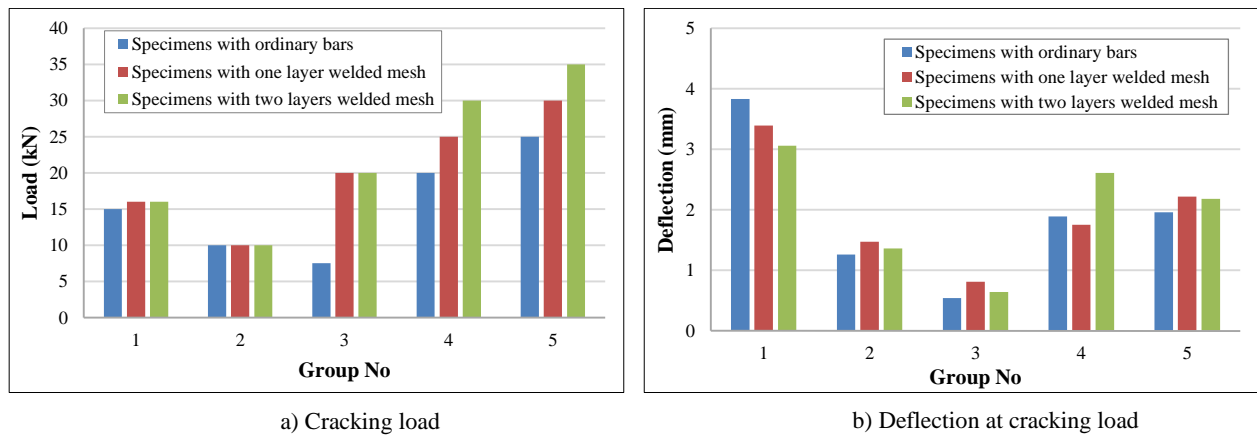

a) Cracking load   b) Deflection at cracking load

Figure 5. Cracking load and deflection results comparison for tested specimens

a) Ultimate load   b) Deflection at ultimate load
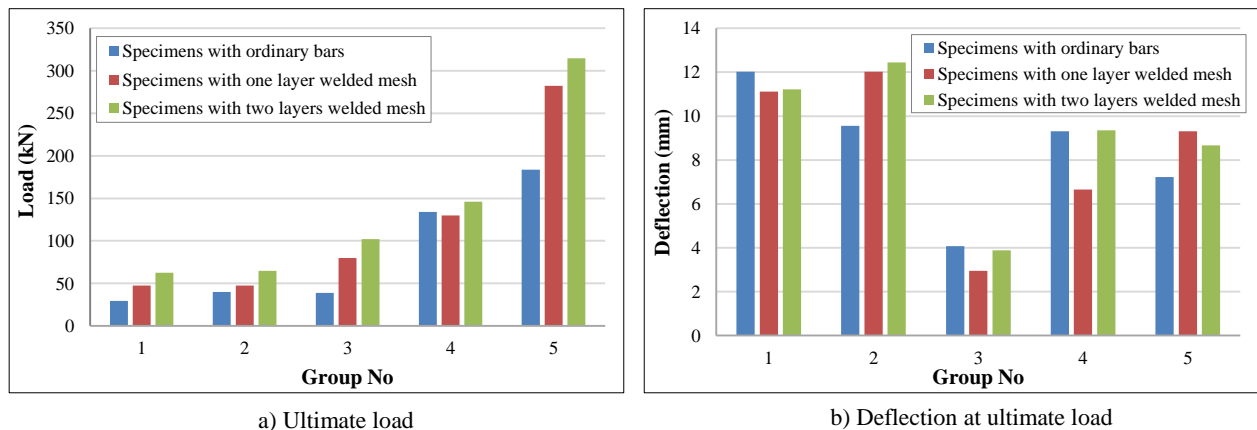
Figure 6. Ultimate load and deflection results for tested specimens

2.6. Reinforcing Steel Strain

Reinforcing steel strains are related to the forces which are transmitted from the applied concentrated load to the lower mesh of steel bars. For Group 1, Group 2, and Group 3, the control specimens RO-S0-CL, RO-S0-LL, and RO-S0-UL recorded the lowest strain due to the fact that the reinforcement bars cross-section in these specimens is larger than the other specimens. However, these specimens failed earlier than the other specimens due to excessive cracking that appeared quickly. Also, specimens with one-layer mesh recorded lower strain than those with two-layer mesh. The data for strain values can be seen in Figure 10 and Table 4. Micro-strain recorded showed that all steel bars reached yield stress.
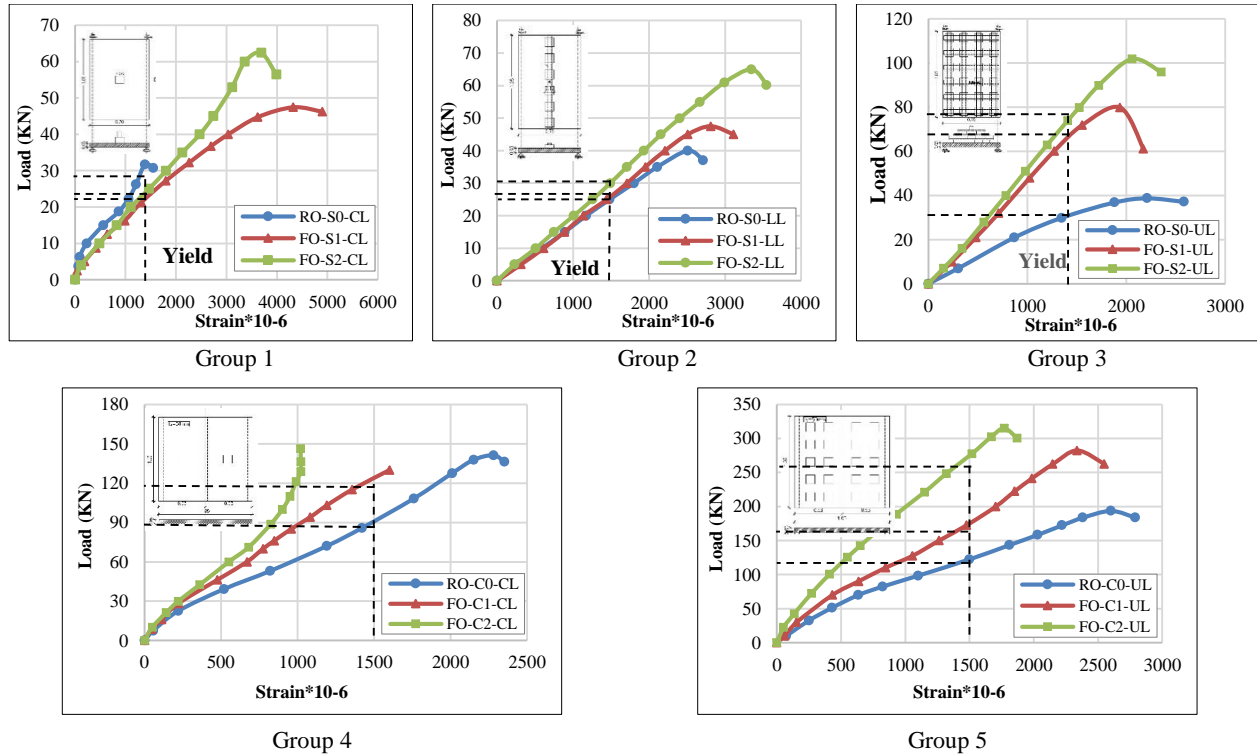

Figure 7. Load–strain curves for all specimens

For continuous slabs subjected to concentrated load, reinforcement in all specimens reached yield strain expected for specimen FO-C2-CL, which was reinforced with two layers of welded mesh. This may be due to damage to the stain gauge during testing or that a punching failure occurred before yielding. For group 5 with continuous slabs subjected to uniform load, reinforcement in all specimens reached yield strain.

3. Finite Element Model

A finite element package (ABAQUS version 6.13) was used to simulate the behavior of the fifteen slabs tested experimentally. ABAQUS is a very complex finite element analysis program introduced with huge material characteristics and parameters to reproduce high accuracy in calculations and provide comprehensive outputs concerning stress analysis. The slabs of the study were modeled as 3D structures in Abaqus. Concrete parts were modeled using C3D8R. The models were divided into fine elements with regular sizes with sizes 50×50×5 mm. Steel bars and metal mesh were modeled using T3D2 elements that were embedded in the surrounding solid elements. Figure 11 shows the modeling of welded and expanded metal mesh in Abaqus. Concrete material was modeled using Abaqus concrete-damaged plasticity model. This model uses the concept of isotropic damage elasticity in combination with isotropic compression and tensile plasticity to model the inelastic behavior of concrete. Tables 5 and 6 present concrete elastic properties and concrete-damaged plasticity model parameters used in the analysis. Steel reinforcement has approximately linear elastic behavior when the steel stiffness introduced by the Young's or elastic modulus keeps constant at low strain magnitudes. At higher strain magnitudes, it begins to have nonlinear, inelastic behavior, which is referred to as plasticity. The plastic behavior of the steel is described by its yield point and its post-yield hardening. The shift from elastic to plastic behavior occurs at a yield point on a material stress-strain curve. The deformation of the steel prior to reaching the yield point creates only elastic strains, which are fully recovered if the applied load is removed. However, once the stress in the steel exceeds the yield stress, permanent (plastic) deformation begins to occur. Both elastic and plastic strains accumulate as the metal deforms in the post-yielding region. The stiffness of the steel decreases once the material yields. The plastic deformation of the steel material increases its yield stress for subsequent loadings. Table 7 shows the elastic properties of steel bars. Figure 12 shows boundary conditions for FE models.
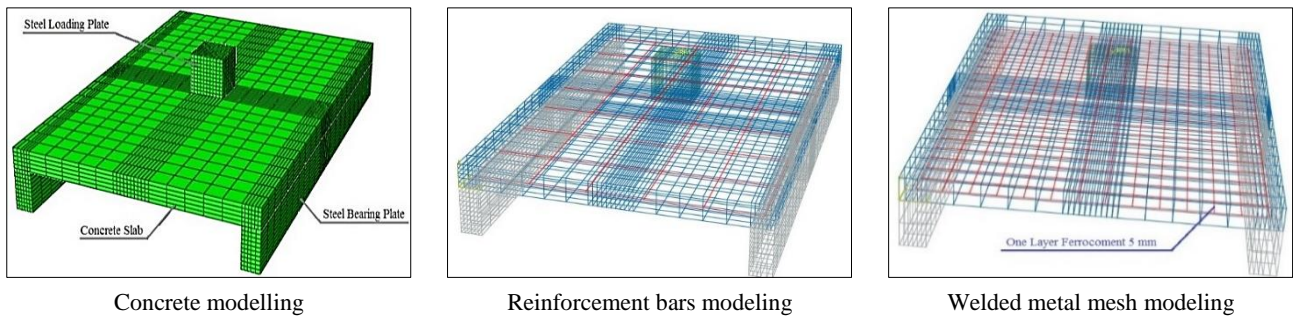
| Concrete modelling | Reinforcement bars modeling | Welded metal mesh modeling |

Figure 8. Modeling of different slabs elements

Table 5. Elastic properties of concrete

Parameter	Value
Density	$2.50 \times 10\text{-}9$ N/mm^3
Modulus of elasticity (E_s)	28500 MPa
Poisson's ratio (υ)	0.20

Table 6. Concrete damaged plasticity parameters

Parameter	Value
Dilation angle	30°
Eccentricity	0.11
f_{b0}/f_{c0}	1.15
K	0.667
Viscosity parameter	0.00
Yield stress in compression	21 MPa
Cross bonding inelastic strain	0.0
Compressive ultimate stress	42 MPa
Cross bonding inelastic strain	0.00158
Tensile failure stress	4.45 MPa

Where: fb0/fc0 is defined as the ratio of initial equi-biaxial compressive yield stress to initial uni-axial compressive yield stress. K is defined as the ratio of the second stress component on the tensile meridian to that on the compressive meridian at initial yield.

Table 7. Material properties of steel reinforcement Φ8

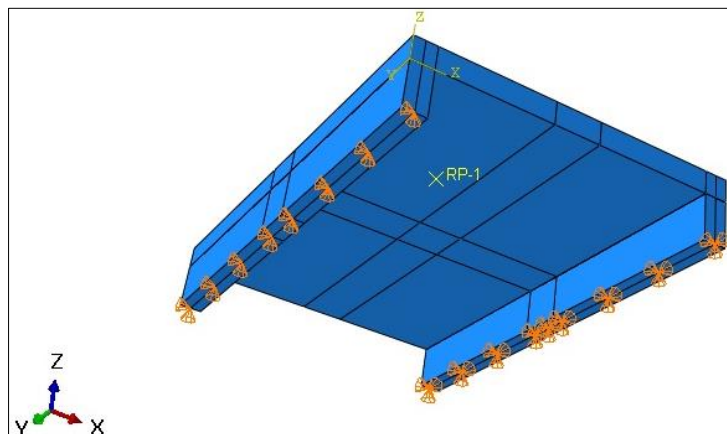| Parameter	Value
Density	7.859×10^{-9} N/mm^3
Modulus of elasticity (Es)	199980 MPa
Poisson's ratio (υ)	0.30
Yield strength	368 MPa
Ultimate strength	537 MPa

Figure 9. Boundary condition of FE models

3.1. Load-Deflection Behavior

Graphical comparisons between the results calculated for all samples using the proposed FEM and the experimental values previously obtained for the load-deflection curves are illustrated in Figures 13 and 14. The numerical predictions of the ultimate capacities were compared against the experimental ones as shown in Table 8, and the difference was at maximum cases within 22% confirming the good performance of the FE model.
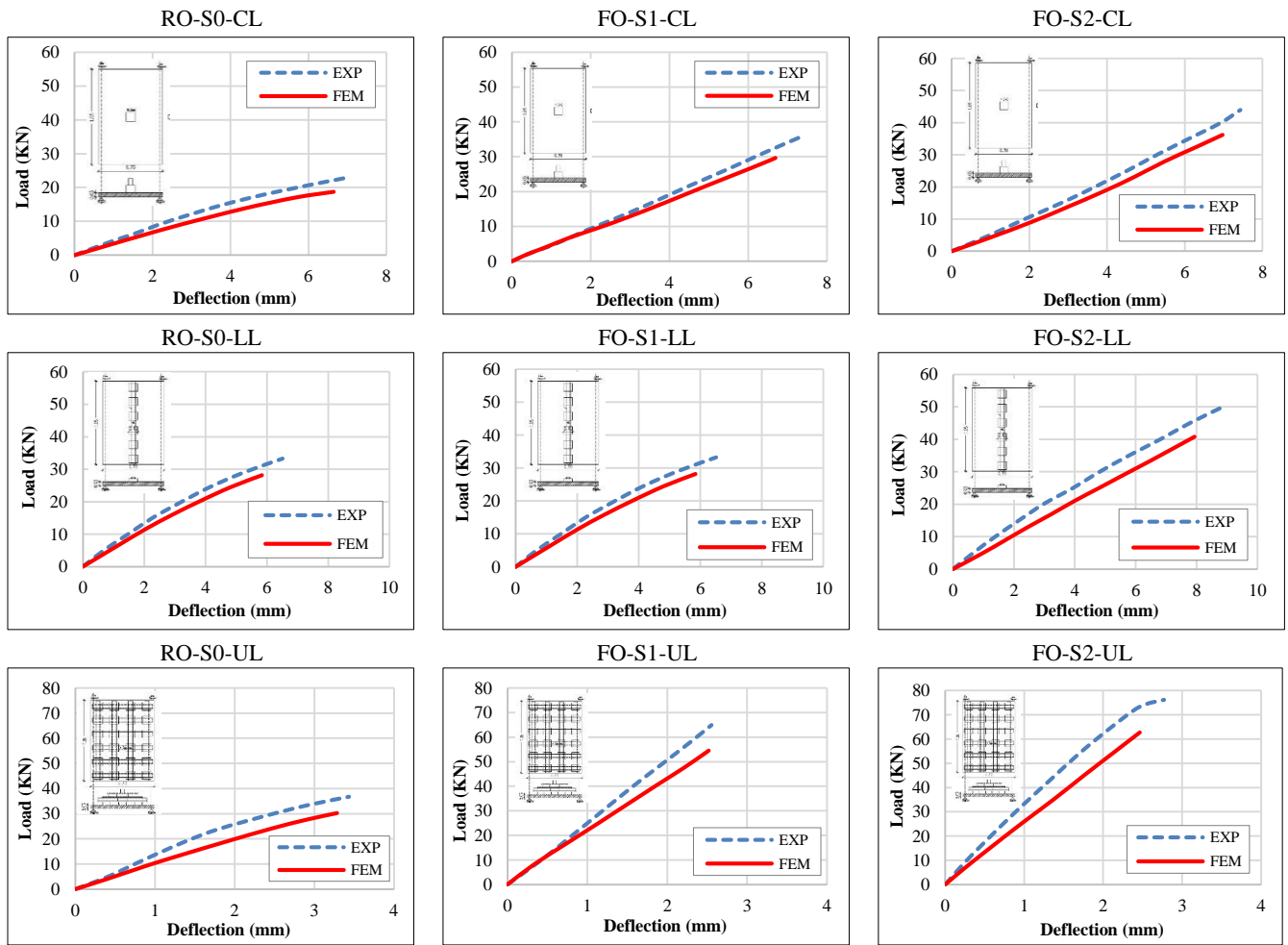

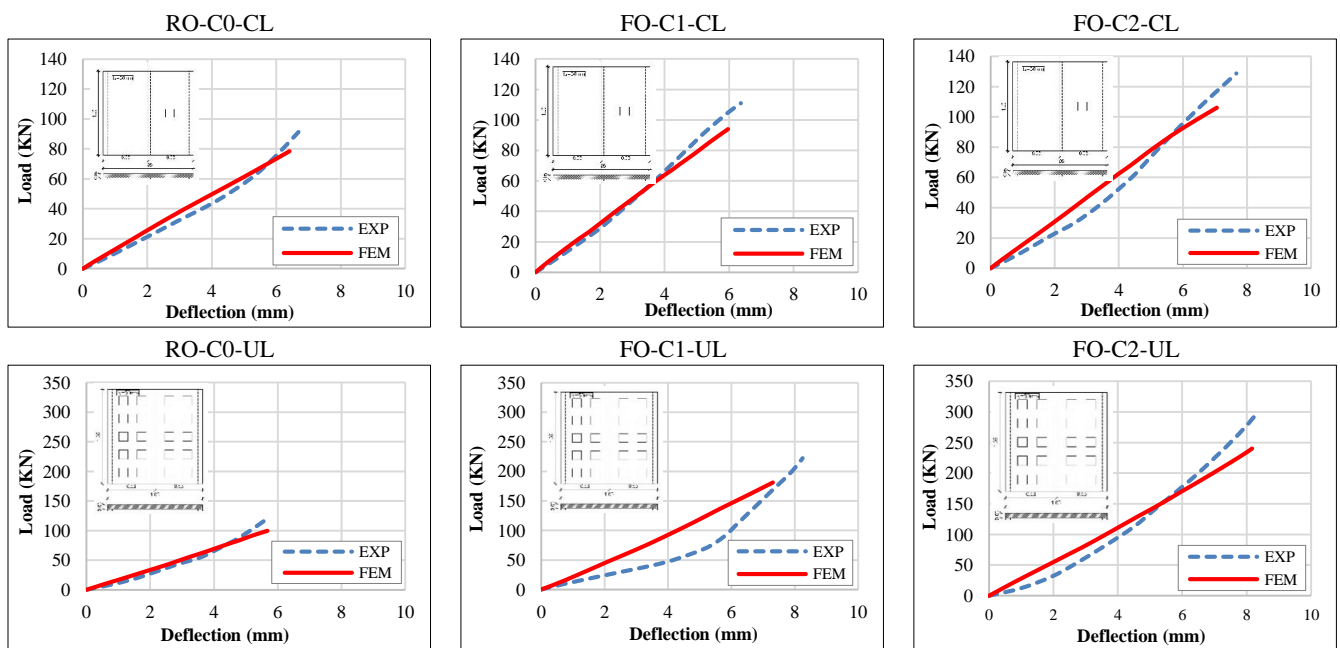Figure 10. Load–deflection curves - comparison between FEM and experiment for simple slabs

Figure 11. Load–deflection curves - comparison between FEM and experiment for continuous slabs

Table 8. Comparison between experimental data and FEM estimation at ultimate load

Group No	Type of Slab	Experimental		Finite Element		% Difference	
		P	Δ	P	Δ	P	Δ
Group 1	RO-S0-CL	22.83	6.95	18.73	6.65	21.89	4.51
	FO-S1-CL	36.22	7.44	29.62	6.69	22.28	11.21
	FO-S2-CL	43.96	7.42	36.16	6.97	21.57	6.46
Group 2	RO-S0-LL	23.98	3.53	21.23	3.23	12.95	9.29
	FO-S1-LL	33.27	6.51	28.17	5.84	18.10	11.47
	FO-S2-LL	49.96	8.86	40.76	7.93	22.57	11.73
Group 3	RO-S0-UL	36.8	3.43	30.27	3.28	21.57	4.57
	FO-S1-UL	64.94	2.55	54.5	2.58	19.16	-1.16
	FO-S2-UL	76.13	2.77	62.74	2.46	21.34	12.60
Group 4	RO-C0-CL	91.2	6.68	78.4	6.41	16.33	4.21
	FO-C1-CL	110.93	6.35	93.94	5.97	18.09	6.37
	FO-C2-CL	128.68	7.66	106.13	7.05	21.25	8.65
Group 5	RO-C0-UL	122.43	5.72	99.72	5.67	22.77	0.88
	FO-C1-UL	222.38	8.24	180.9	7.3	22.93	12.88
	FO-C2-UL	292.35	8.24	240.35	8.17	21.64	0.86

The deviation between numerical and experimental results can be explained as follows:

- Good bond at the elastic stage was assumed by modeling steel reinforcement as an embedded element in the concrete host element, and bond degradation factor was taken into consideration at the plastic stage and was derived from empirical equations. This assumed factor may differ from experimental study to another and needs more studies.

- Modeling concrete compressive and tensile stress-strain properties using theoretical descriptive equations depending on the 28 days cube compressive strength values may differ slightly from the actual stress-strain behavior of concrete cast at lab conditions and testing.

3.2. Load-Steel Strain Behavior

Results from the numerical FEM are compared with readings on strain gauges recorded during loading in the experimental program. In general, the results show a good correlation between the FEM and the experimental results. Values from the numerical analysis are slightly lower than the ones obtained from laboratory tests as shown in Figures 15 and 16. For Group 1 (simple slabs loaded by concentrated load), all specimens reached yield strain and failed due to flexural failure as severe cracks appeared. For Group 2 and Group 3 (simple slabs loaded by line and uniform load), the experimental and finite element curves are close to each other at the first stage of loading, and by increasing the load, the curves diverge, especially under uniform load due to loading conditions. For Group 4 (continuous slabs loaded by concentrated load), the experimental and finite element curves are close to each other, except for specimens with two welded meshes where punching failure was observed in the experimental data. For Group 5 (continuous slabs loaded by uniform loads), the load-strain curve behaves non-linearly where all specimens reach yield strain.
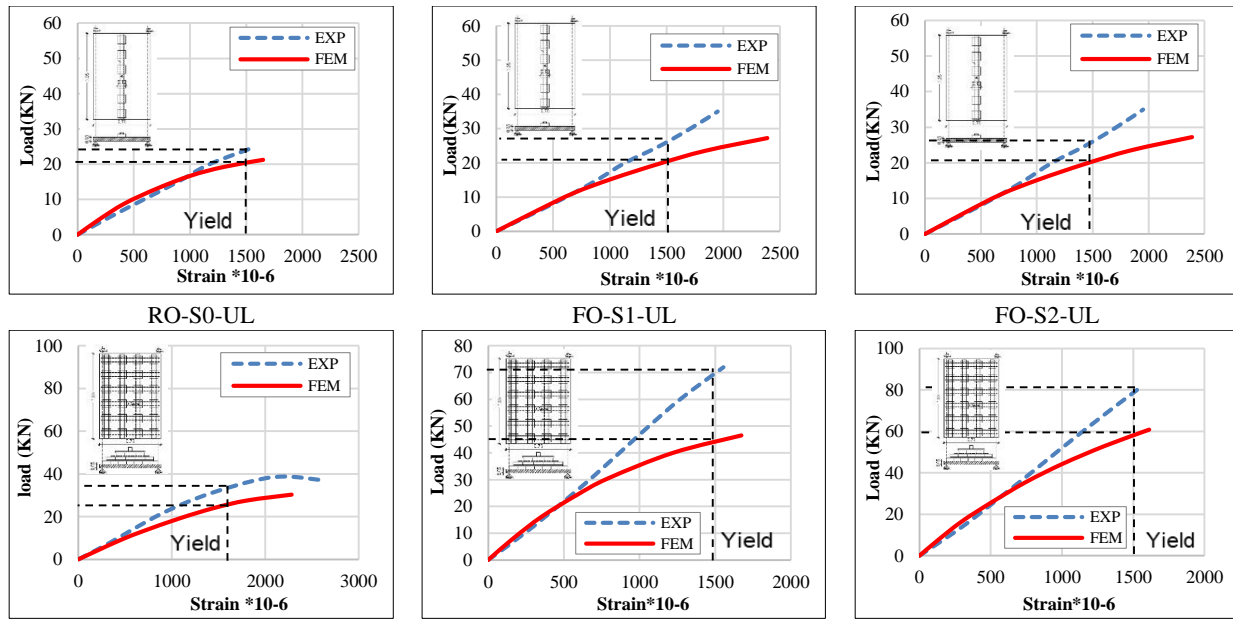

RO-S0-CL   FO-S1-CL   FO-S2-CL

RO-S0-LL   FO-S1-LL   FO-S2-LL

RO-S0-UL   FO-S1-UL   FO-S2-UL
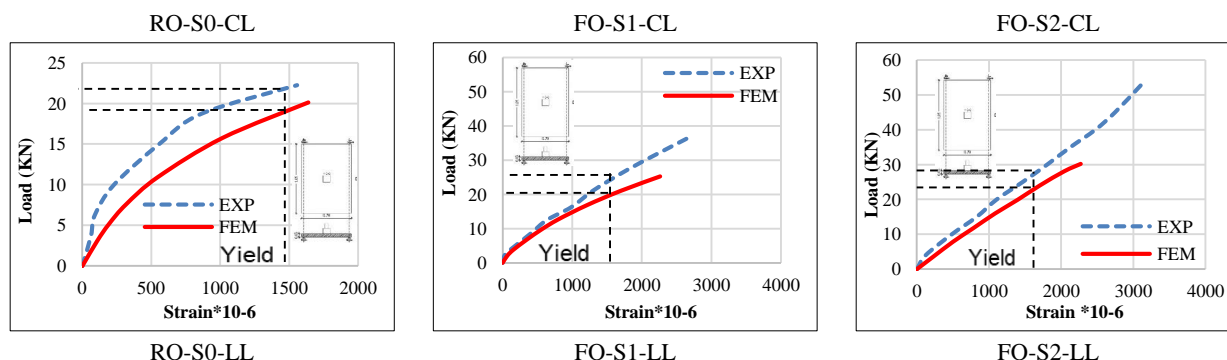
Figure 12. Load–strain curves - comparison between FEM and experiment for simple slabs

RO-C0-CL   FO-C1-CL   FO-C2-CL

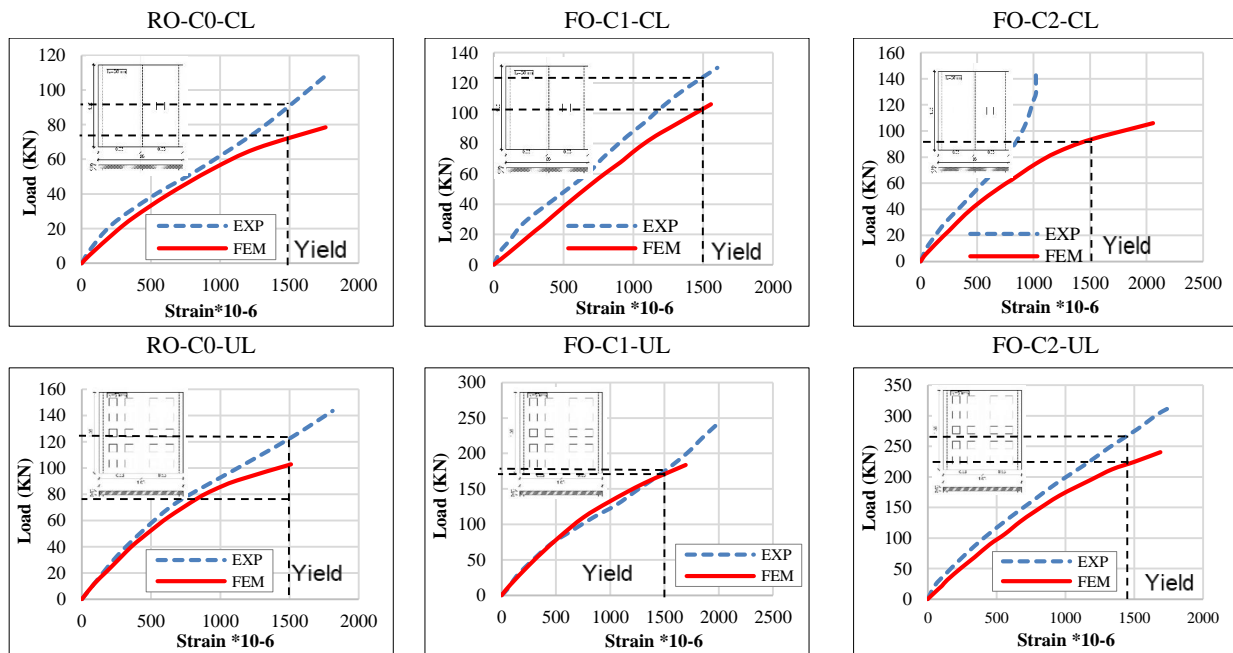RO-C0-UL   FO-C1-UL   FO-C2-UL

Figure 13. Load–strain curves - comparison between FEM and experiment for continuous slabs

3.3. Mid-Point Displacement

The displacement of the mid-point of the specimen was one of the most important outcomes that has been relied upon in predicting specimen rigidity and strength. The mid-point of the specimen was specifically selected as it is the location where the maximum deflection occurred. Figures 13 and 14 illustrate the relationship between applied load and deflection, which is recorded every 5 kN and recorded by the data acquisition system. The displacement was large for concentrated load (group 1), which was acting on the mid span and recorded 7.44 mm at ultimate load, and small for uniform load (group 3), which was distributed on the top face of the slab and recorded about 3.43 mm at ultimate load. The relationship obtained by Abaqus for the same slab is shown in Figures 13 and 14. Table 8 and Figure 17 show a comparison of the final values of the mid-point displacements for the fifteen specimens that were tested. They were measured and analyzed.
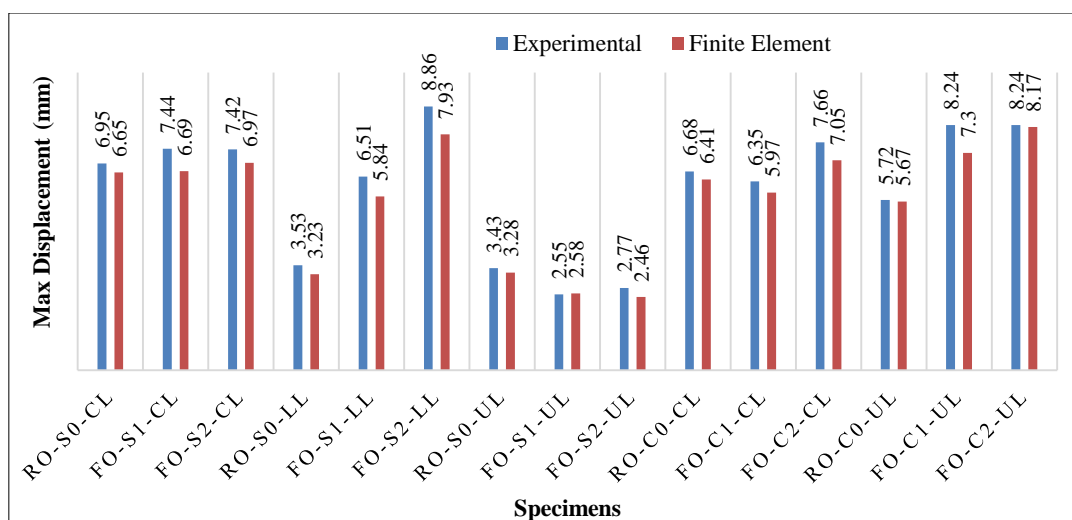
Figure 14. Max displacements comparison

Generally, there is good agreement between experimental and numerical results for the maximum displacement, with a mean value of 7% difference. It can be observed that for specimens loaded under concentrated load, the deflection values increase by adding welded metal mesh, either one layer or two layers, and the difference between experimental and numerical results increases and reaches 11.21% for a one-layer metal mesh specimen. For specimens loaded under line load, the deflection values increase by adding welded metal mesh, either one layer or two layers. The difference between experimental and numerical increases reaches about 11.50% for both one- and two-layer metal mesh specimens. Slabs loaded by uniform load give a different behavior where the deflection values decrease by adding welded metal mesh, either one layer or two layers, and this may happen due to arch action.

3.4. Cracked Pattern

As expected, cracks appeared at the lower surface of specimens (tension zone), as shown in Figure 5. A failure zone is localized under the point where concrete has completely collapsed and then cracks spread gradually by moving away from that zone. Cracks appeared with remarkable width near the failure zone and turned into very fine cracks until reaching supports. In addition to predicting the ability of the specimen to absorb load energy, the failure pattern gives an indication of how the specimen was affected by load type, which contributes to finding some methods that increase the strength of the slab and reduce the size of the failure zone. Figures 5 and 6 show the cracked patterns of tested specimens for all groups. Obviously, specimens with added metal mesh, in general, had smaller cracked widths compared to slabs with steel bars.

4. Conclusions

The effect of welded and expanding reinforcing metal mesh on the behavior of slabs under different types of loading has been experimentally and numerically investigated in the present study. Nine one-way simple specimens and six continuous one-way slabs with two equal spans were prepared and tested in the Faculty of Engineering, Cairo University, Egypt. Based on the test results, the following conclusions can be drawn as follows:

- Adding welded wire mesh in concrete led to a more ductile behavior for the tested slab under flexural loads. Welded wire mesh can be used in RC slabs as an alternative material to ordinary steel bars.

- Using welded mesh in concrete delayed the cracks' appearance and decreased crack width, which meant the cracks grew slowly and with better distribution. Using welded wire mesh as an alternative to ordinary reinforcing bars can significantly improve the ultimate capacity of slabs. For simple one-way solid slabs, using welded wire mesh increased the slab loading capacity by about 61% for concentrated load, 19% for line load and 100% for uniform load compared to slabs reinforced with ordinary bars.

- For continuous one-way solid slabs, using welded wire mesh decreased the slabs' loading capacity by about 3.20% for the concentrated load as punching failure occurred before flexural failure and increased the capacity by about 53.70% for uniform load compared to slabs reinforced with ordinary bars.

- Additional welded wire mesh with the same diameter and spacing as the main mesh increased the carrying loading capacity for slabs by about 27–36% over those with only one layer.

- The loading setup for uniform loading caused an arch action, which led to an increase in the load capacity of the specimens. This needs further investigation with spans greater than one meter to provide a better loading setup. The FE model provides an acceptable level of accuracy where the numerical predictions of the ultimate capacities are close to the experimental ones, confirming the good performance of the FE model.

5. Declarations

5.1. Author Contributions

5.2. Data Availability Statement

The data presented in this study are available in the article.

5.3. Funding

5.4. Conflicts of Interest

The authors declare no conflict of interest.

6. References

[1] ACI 439.5R. (2018). Guide for the Specification, Manufacture, and Construction Use of Welded Wire Reinforcement. American Concrete Institute (ACI), Michigan, United States.

[2] Naser, F. H., Al Mamoori, A. H. N., & Dhahir, M. K. (2021). Effect of using different types of reinforcement on the flexural behavior of ferrocement hollow core slabs embedding PVC pipes. Ain Shams Engineering Journal, 12(1), 303-315. doi:10.1016/j.asej.2020.06.003.

[3] Ali, Z. M., Hama, S. M., & Mohana, M. H. (2020). Flexural behavior of one-way ferrocement slabs with fibrous cementitious matrices. Periodicals of Engineering and Natural Sciences, 8(3), 1614-1624. doi:10.21533/pen.v8i3.1548.

[4] Allawi, A. A., & Ali, S. I. (2020). Flexural Behavior of Composite GFRP Pultruded I-Section Beams under Static and Impact Loading. Civil Engineering Journal, 6(11), 2143–2158. doi:10.28991/cej-2020-03091608.

[5] Leeanansaksiri, A., Panyakapo, P., & Ruangrassamee, A. (2018). Seismic capacity of masonry infilled RC frame strengthening with expanded metal ferrocement. Engineering Structures, 159, 110-127. doi:10.1016/j.engstruct.2017.12.034.

[6] Li, J., Wu, C., & Liu, Z.-X. (2018). Comparative evaluation of steel wire mesh, steel fibre and high performance polyethylene fibre reinforced concrete slabs in blast tests. Thin-Walled Structures, 126, 117–126. doi:10.1016/j.tws.2017.05.023.

[7] Shaheen, Y. B. I., Hekal, G. M., & Fadel, A. K. (2018). Experimental and numerical study of the behavior of RC slabs with openings reinforced by metal mesh under impact loading. Challenge Journal of Concrete Research Letters, 9(2), 37-51. doi:10.20528/cjcrl.2018.02.001.

[8] Shaheen, Y. B. I., & Eltehawy, E. A. (2017). Structural behaviour of ferrocement channels slabs for low cost housing. Challenge Journal of Concrete Research Letters, 8(2), 48-64. doi:10.20528/cjcrl.2017.02.002.

[9] ECO 203. (2018). Egyptian Building Code for Structural Concrete Design and Construction, Ministry of Housing Utilities and urban Communities, Cairo, Egypt.

[10] ESS, 4756-11. (2007). Physical and mechanical properties examination of cement, part 1. Egyptian Standards Specification, Cairo, Egypt.

[11] Işıkdağ, B. (2015). Characterization of lightweight ferrocement panels containing expanded perlite-based mortar. Construction and Building Materials, 81, 15–23. doi:10.1016/j.conbuildmat.2015.02.009.

[12] Ibrahim, H. M. (2011). Experimental investigation of ultimate capacity of wired mesh-reinforced cementitious slabs. Construction and Building Materials, 25(1), 251–259. doi:10.1016/j.conbuildmat.2010.06.032.

[13] ACI 440.1R-06. (2006). Guide for the design and Construction of Structural Reinforcement with FRP Bars. American Concrete Institute (ACI), Michigan, United States.

[14] ACI 549R-97. (1997). State-of-the-Art on ferrocement. American Concrete Institute (ACI), Michigan, United States.

[15] ASTM C1116/C1116M-10a. (2015). Standard Specification for Fiber-reinforced Concrete. ASTM international, Pennsylvania, United States.

[16] ASTM C494/C494-08. (2017). Standard Specification for Chemical Admixtures for Concrete. ASTM international, Pennsylvania, United States.